HMT MODELLING OF EXTERIOR WALLS SUBMITTED TO HARSH TEST CONDITIONS

HMT-MODELLIERUNG VON AUßENWÄNDEN UNTER HARTEN TESTBEDINGUNGEN

Nayara Sakiyama, Jürgen Frick, Harald Garrecht

Materials Testing Institute (MPA), University of Stuttgart, Otto-Graf-Institute

SUMMARY

This paper investigates the hygrothermal performance of walls with external insulation render. An aerogel-based material was considered, which was developed and characterized in the framework of the Horizon-2020 project 'Wall-ACE'. The methodology followed the development of 2D heat and moisture transfer (HMT) models, calibrated for measured temperature and heat flux data from a large-scale artificial weathering laboratory test. Four different exterior wall structures were considered as a result of combining two external insulation renders applied to both concrete blocks and hollow bricks as support walls. Besides describing the calibration process, this research also considers the relationship between impedance measurements and the moisture content calculated by the numerical model. Although the simulated values have more stable behaviour than the impedance measured, due to the extreme conditions of the EOTA test that are hardly reproduced by the numerical model, the results showed a direct relationship between both considered parameters. The innermost layer of the external insulation render, close to the support walls presented the higher moisture content as well as the lowest impedance readings.

ZUSAMMENFASSUNG

In diesem Beitrag wird die hygrothermische Leistung von Wänden mit Außendämmputz untersucht. Es wurde ein Material auf Aerogel-Basis betrachtet, das im Rahmen des Horizon-2020-Projekts 'Wall-ACE' entwickelt und charakterisiert wurde. Das Verfahren folgte der Entwicklung von 2D-Wärme- und Feuchtigkeitstransportmodellen (HMT), die für gemessene Temperatur- und Wärmestromdaten aus einem groß angelegten künstlichen Bewitterungslabortest kalibriert wurden. Es wurden vier verschiedene Außenwandstrukturen betrachtet, die sich aus einer Kombination von zwei Außendämmputzen ergaben, die sowohl auf

Betonblöcke als auch auf Hohlziegel als Stützmauern aufgebracht wurden. Neben der Beschreibung des Kalibrierverfahrens wird auch die Beziehung zwischen Impedanzmessungen und dem durch das numerische Modell berechneten Feuchtigkeitsgehalt betrachtet. Obwohl die simulierten Werte ein stabileres Verhalten aufweisen als die gemessene Impedanz, zeigten die Ergebnisse aufgrund der extremen Bedingungen des EOTA-Tests, die durch das numerische Modell kaum wiedergegeben werden, eine direkte Beziehung zwischen den beiden betrachteten Parametern. Die innerste Schicht des äußeren Dämmputzes in der Nähe der Stützwände wies sowohl den höheren Feuchtigkeitsgehalt als auch die niedrigsten Impedanzwerte auf.

1.   INTRODUCTION

Awareness related to building performance follows the worldwide concern to achieve sustainable goals. In this sense, the European Union (EU) has demanded a 27% improvement in the energy efficiency of buildings by 2030 [1]. This movement has encouraged the development of high-performance insulation materials, such as silica-aerogel based insulating systems. One of the building applications regarding aerogel granulate is a mixture with plasters and renders, which have excellent thermal performance (thermal conductivity between 0.026 W/(mK) and 0.030 W/(mK)) [2, 3].

Moreover, although energy efficiency is a key factor related to insulating materials, its hygric performance configures an essential feature of building envelope design. Moisture problems can lead to mould growth, pour indoor air quality, metal corrosion, wood decay, besides thermal resistance losses [4]. Therefore, the hygrothermal behaviour of exterior walls has been the focus of investigations that try to assess moisture content, condensation risks and other possible decay [5–7]. Most of these studies are accompanied by numerical models that simulate coupled HMT, which are usually supplemented by experimental observations [8] or laboratory tests [9] to validate/calibrate the model.

When comparing simulation results and measurement data related to hygrothermal assessments, one might give special attention to the boundary conditions and material properties [10] involving the phenomena. They directly impact the outputs, and the more they are known, the better the reliability of the generated model. A detailed approach in conducting this process can be found in [11], which consider the uncertainties and possible biases that can not be avoided. Besides,

parametric analyses [12] and optimization tools [13] are systematic and reproducible procedures that can assist model development and thus lead to better accordance with the measurement outcomes.

In this study, the focus is at the hygrothermal performance of exterior walls, which are covered with high-performance insulation render for new or retrofitted buildings. The methodology included performing a large-scale monitored test under controlled conditions, which was equipped with hygrothermal and impedance sensors. From these experimental data, a numerical model was developed and calibrated. Finally, the performance of the walls is assessed by comparing the impedance measurements to the simulated water content.

2. HMT MODEL

2.1 EXPERIMENTAL MONITORING CAMPAIGN

An aerogel-based insulating external render was developed in the framework of the Horizon 2020-project "Wall-ACE" [14]. The structural and hygrothermal behaviour of the product was assessed through a large-scale laboratory test (EOTA-wall test) according to DIN EN 16383:2017 [15], which is usually used to evaluate ETICS[1] systems and serves as a test with harsh conditions.

> Back wall: Concrete Blocks (495x240x248 mm)
> Adhesion layer at concrete blocks
> **Exterior insulation render layer** (2 layers 25 mm each)
>   . Aerogel-based/Wall-ACE Project (left side)
>   . TRI-O-THERM M (right side)
> Base coat with glass fiber mesh
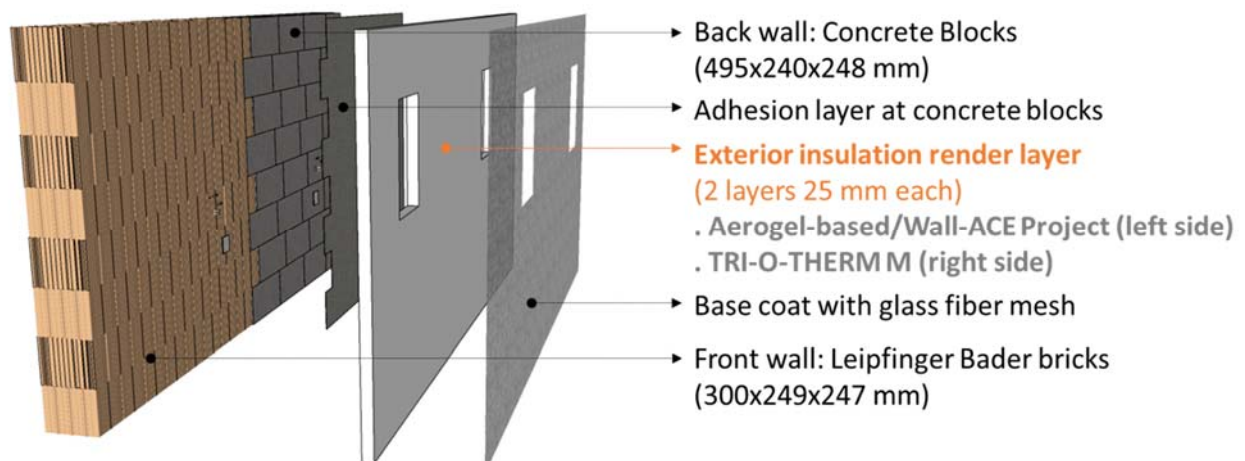> Front wall: Leipfinger Bader bricks (300x249x247 mm)

Fig. 1: EOTA Wall construction sketch

The EOTA chamber is composed of two envelope/walls, built in the lab and enclosed by a sealing system (doors, floor and ceiling). Assessed walls of 4.0 x 2.1 m (length x height) face each other, separated by 1 m. Each opposing partition

---

[1] External thermal insulation composite systems (ETICS)

was constructed with both bricks and concrete blocks. The Wall-ACE project aerogel-based exterior render was applied on one side, while another high-tech perlite-based render (Tri-O-Therm) was used on the other side as reference material (Fig. 1). The combination of support materials and external renders used at the large scale test resulted in four wall configurations, listed in Table 1.

Table 1: EOTA-wall test, Wall assembly configurations

Investigated Wall	Support material	Outside Render	U-value [16] (W/m².K)
A	Hollow brick	Aerogel	0.198
B	Hollow brick	Tri-O-Therm	0.232
C	Concrete Block	Aerogel	0.377
D	Concrete Block	Tri-O-Therm	0.508

Two bricks and two concrete blocks, one at each wall type, were equipped with different sensors in different positions (Fig. 2). Impedance sensors, which consist of two probes (screws) surrounded with a conducting rubber at a proximity distance of 1,5 cm, were incorporated in the bricks, joints and exterior render. Parallel to the impedance sensors, hygrothermal sensors (Sensirion SHT 25) were fixed and covered with a porous tube or with a glass fibre tape. Furthermore, heat flux sensors (ALMEMO FQA0xx) were also installed at the tested walls. A detailed description of the test weathering cycles, wall construction, as well as the temperature and heat transfer monitoring can be found in [16].
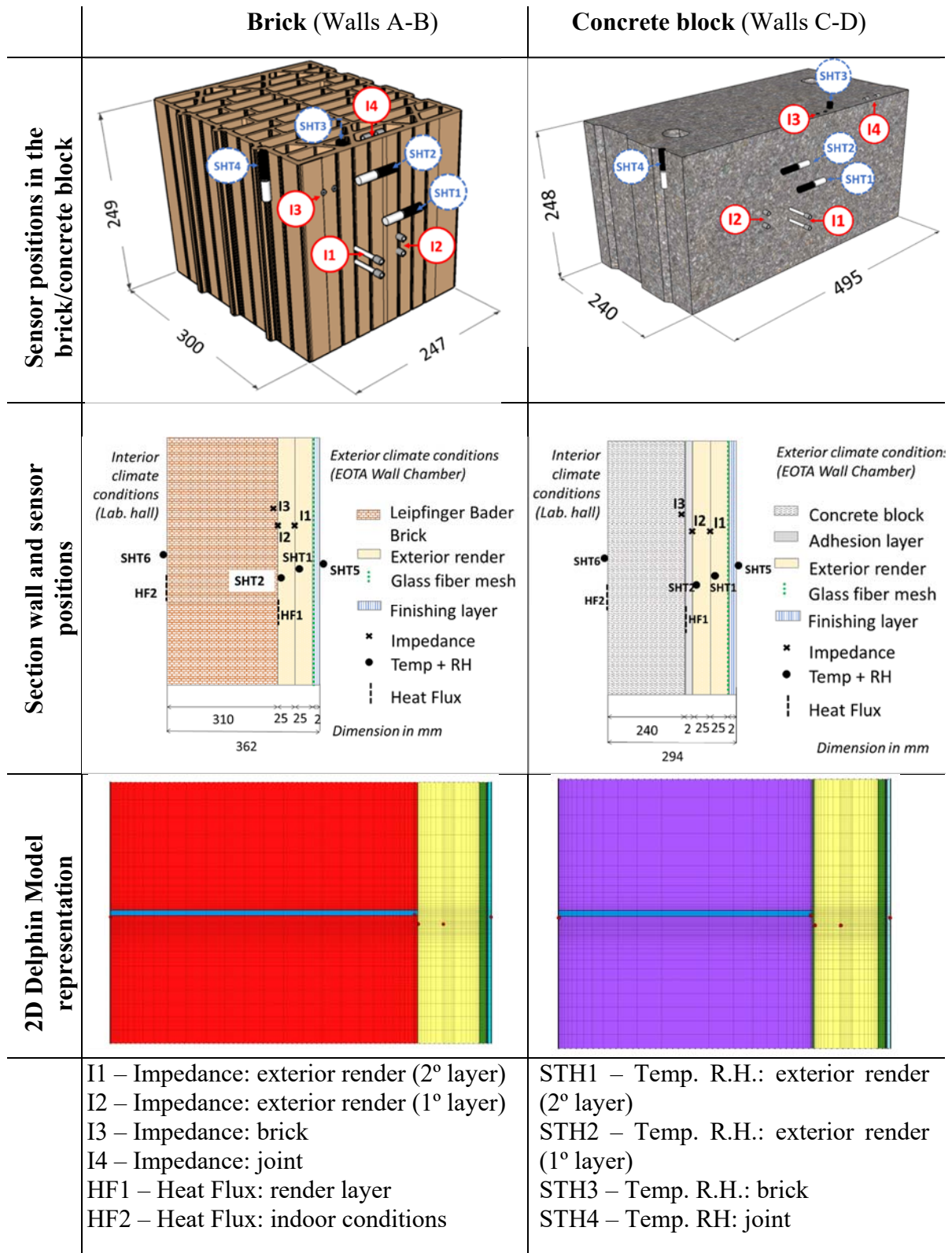
Brick (Walls A-B)	**Concrete block** (Walls C-D)
Sensor positions in the brick/concrete block	
Section wall and sensor positions	
2D Delphin Model representation	
I1 – Impedance: exterior render (2º layer) I2 – Impedance: exterior render (1º layer) I3 – Impedance: brick I4 – Impedance: joint HF1 – Heat Flux: render layer HF2 – Heat Flux: indoor conditions	STH1 – Temp. R.H.: exterior render (2º layer) STH2 – Temp. R.H.: exterior render (1º layer) STH3 – Temp. R.H.: brick STH4 – Temp. RH: joint

Fig. 2: Brick/Concrete block sketches – sensor position

2.2 THE NUMERICAL MODELS

The software Delphin 6.1 [17] was used to solve the transient coupled two-dimensional heat and moisture transport in the multi-layer EOTA test walls. Delphin complies with the standard EN 15026 [18], and it was used in several studies to assess the hygrothermal performance of building façades [19, 20].

Input model variables and functions include the following:

- Boundary conditions/Interfaces (outdoor climate + indoor environment, surface transfer coefficients);

- Construction element dimensions and material properties of each layer (moisture/liquid water storage and transport functions);

- Surface orientation and inclination;

- Output files (ex: temperature, RH and moisture content profiles);

- Initial conditions (temperature and moisture content);

- Start time and duration of the simulation.

In Fig: 3 the boundary conditions are shown. The external climate corresponds to the controlled EOTA test weathering cycles, while the interior environment is the recorded free-float temperatures and relative humidity inside the testing warehouse where the EOTA chamber stands. Wind-driven rain (imposed flux - l/m²h) was also considered as an external boundary condition since water is sprayed at some of the test cycles. However, the water flow was not monitored and, therefore, the input values were based on the standard data and the temperature and RH measured inside the EOTA chamber.
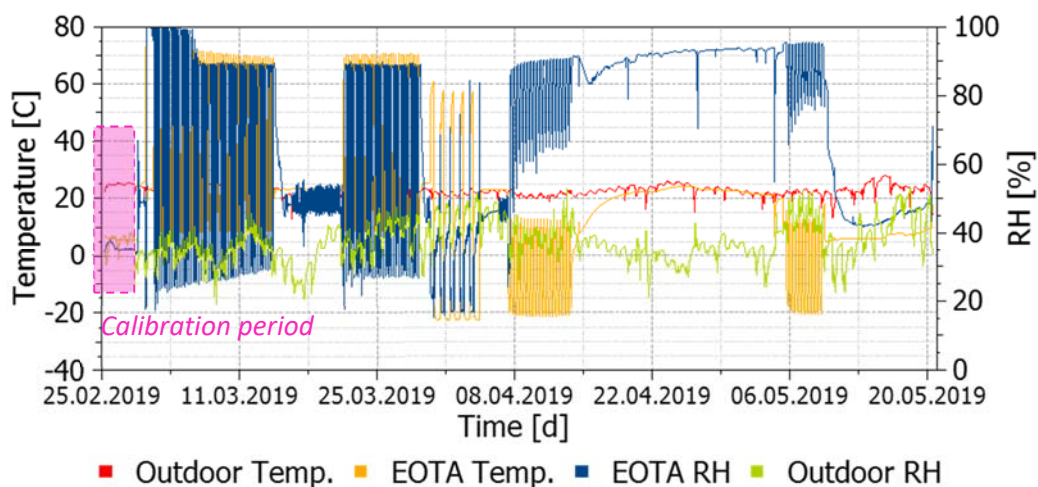

Fig: 3: Exterior boundary conditions (EOTA test chamber) and interior boundary conditions (measured temperature and relative humidity inside the testing warehouse)

The hygrothermal and physical characteristics of the Wall-ACE external render are presented in Table 2, and they were measured by the project associates at both Material Testing Institute and Politecnico di Torino. Its thermal conductivity was measured by means of a guarded hot plate and heat flow meter according to the DIN EN 12667 standard [21]. Its specific heat was measured according to the ASTM C1784 standard [22] through the adoption of the Dynamic Heat Flux Meter (Lasercomp FOX 600). As for the density and porosity values, the measurements followed the DIN EN 1602 standard [23] and DIN EN ISO 8130-2 standard [24] respectively. Finally, its vapour diffusion resistance factor was measured using the Cup method according to the DIN EN ISO 12572 standard [25] and the water absorption to the DIN EN 1015-18 [26].

Table 2: Thermo-physical properties of the Wall-ACE aerogel-based insulating rendering

| Thermal conductivity (λ: W/mK)	0.03 (10°C, dry)
Specific heat (Cp: J/kgK)	940
Density (ρ: kg/m³)	170
Porosity (%)	60
Vapour diffusion resistance factor (-)	2
Water absorption coefficient (kg/m²s$^{1/2}$)	0.76336

All four walls were modelled according to Fig. 2 — the concrete blocks as a 5-layer component and the brick walls as a 4-layer component, with the same section thickness and block height. Also, a 5 mm vertical mortar joint between the blocks was considered, splitting each total block height in two, which lead to a 2D model. The material properties of the single layers composing the walls, except for the aerogel-based external render, were not directly measured, so they were selected from the Delphin materials database, following the properties of the ones used at the EOTA test. The detailed material features can be found in [16].

Finally, the space discretization was defined through the automatic software subdivision option, and subsequently, the grid was refined near to the point where the sensors were installed at the walls. The simulation time step was settled to 15 min (monitoring frequency), and the output data is equivalent to the measured one: temperature (°C)/SHT1-4, heat flux (W/m²)/HF1-2 and moisture content (kg)/Impedance.

2.3   MODEL CALIBRATION

Preliminary validation based on a trial and error approach was performed confronting the numerical simulation results against the experimental measurements carried out within the EOTA wall test. All sensors outlined in Fig. 2 were used as control points, exceptionally for the SHT4, installed aside bricks. Time-series and scatter plots from measured versus simulated results were plotted as a simple way to verify discrepancies in the model. For these initial calibration process, the first seven days of the experiment were used (highlighted in Fig: 3), which characterizes a period before the test cycles begin and therefore is more stable, allowing a better tuning of the calibration process.

Most of the input variables and functions, with the exception of the imposed water flux, had a low uncertainty range since detailed information of the boundary conditions, and material properties were available. Therefore, no statistical calibration step was performed, and minor one-off changes in the model were enough to improve the relation between simulation and measurements results. For the sake of space, Fig. 4b shows some of the results of Wall A (Brick+Aerogel) plotted as dispersion surrounding a y=x line with their respective coefficient of determination (R^2). The maximum and minimum difference from HF2 is shown as time-series in Fig. 4a.
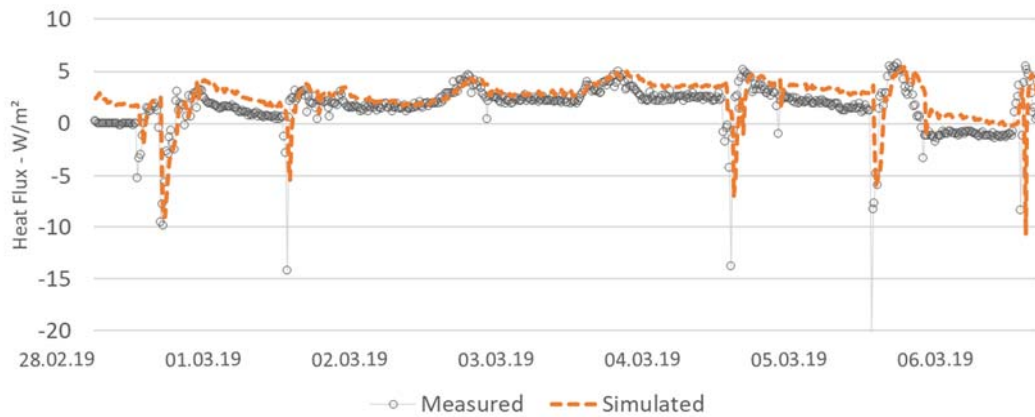
a) Wall A - HF2 time-series
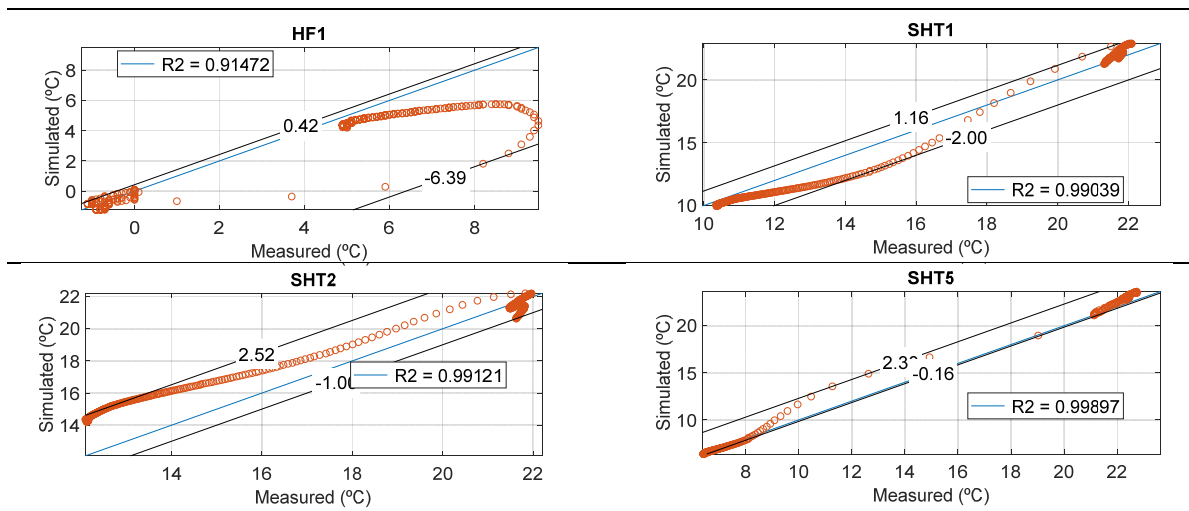
b) Wall A – scatter plots

Fig. 4: Simulated vs measured data of Wall A. a) HF2 time-series, b) scatter plots

Furthermore, the Coefficient of Variation of the Root Mean Square Error (%) - CV (RMSE) was calculated for each control point, set out by ASHARE Guideline 14 [27]. The dimensionless indices correlating predicted and measured data for each sensor are summarised in Table 3.

The standard is the current internationally accepted criteria to quantify the degree of (dis) agreement between recorded data and whole energy model responses. The simulation model is considered 'calibrated' for CV RMSE values up to 15%, for monthly measured data, or 30%, for hourly measured data. While a lack of specific standards for calibration criteria remains and there is no specific one addressing hygrothermal models, the tolerable error interval specified by the document is used here as a reference parameter to determine whether the model can be considered calibrated or not. As the model calibration records and simulation outputs in this study were sampled in a 15 min time step, hourly criteria are used as the acceptance threshold.

Table 3: CV RMSE (%) values for each control point

	CONTROL POINTS	HF1	HF2	SHT1	SHT2	SHT3	SHT5	SHT6
WALLS	A	0.36	*-3.21*	0.05	0.11	0.12	0.04	0.03
	B	0.43	*-3.82*	0.06	0.15	0.12	0.08	0.02
	C	0.30	*-2.10*	0.06	0.12	0.06	0.10	0.02
	D	0.27	*-2.41*	0.12	**0.37**	0.06	0.04	0.03

It is observed that the CV RMSE of the SHT sensors (temperature measurements) falls under the index of the ASHARE Guideline 14, with the exception of the SHT2 of the Wall D. The variation between monitored and measured data is less than 10% for the sensors installed in the most external layers, with bigger discrepancies when getting deeper into the wall assembly. The higher CV RMSE values of the heat flux density, especially for the plate installed on the outer wall of the test chamber, are justified due to its location. The boundary conditions are inconstant since the room environment is not controlled, workers move around, and openings remain in operation, causing large divergences between measured and simulated values.
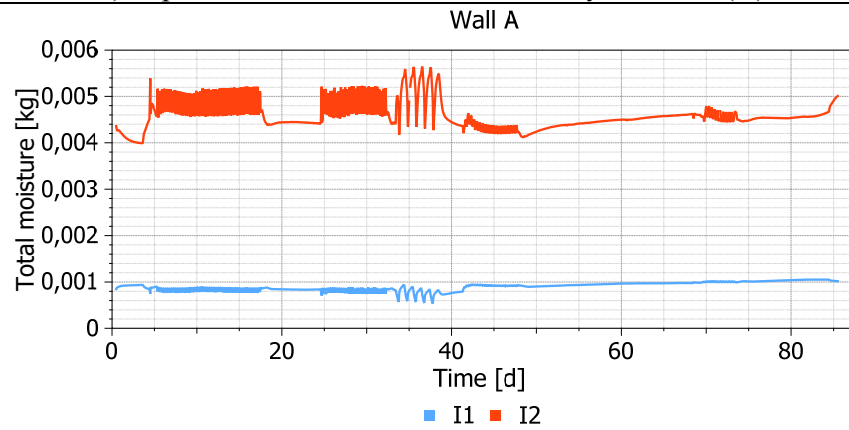
3.   IMPEDANCE X MOISTURE CONTENT

Simulated total moisture mass density (kg) over the test period was compared to the impedance measurements (Ω) at two insulation depths. Fig. 5 and Fig. 6 show the results of the walls covered with aerogel-based exterior render (Walls A and C) and the walls that received Tri-O-Therm (Walls B and D) are shown in Fig. 7 and Fig. 8. The red/dark line corresponds to the measurements taken near the support material surface (I2) on the innermost layer of the external insulation render, while the blue/light line refers to the measurements located on its outer edge (I1), see Fig. 2. Impedance readings appear with an inverted Y-axis to propitiate a direct relationship with the total moisture mass density output from the Delphin model, since higher impedance values are related to lower water content, and vice-versa.

Wall A (brick + aerogel)
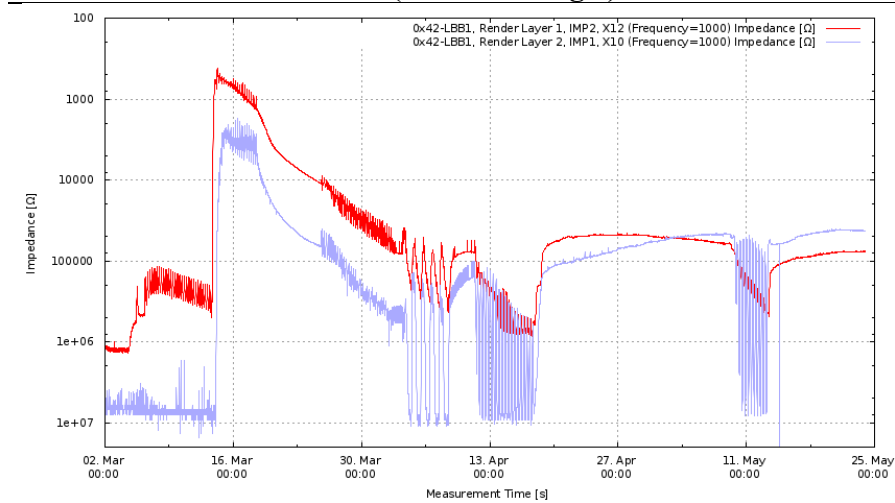
a) Impedance measurements:insulation layer – I1, I2 (Ω)

b) Delphin output - Moisture content (kg) at the same control points

Fig. 5: Moisture content over time in Wall A. a) Impedance measurements I1, I2,
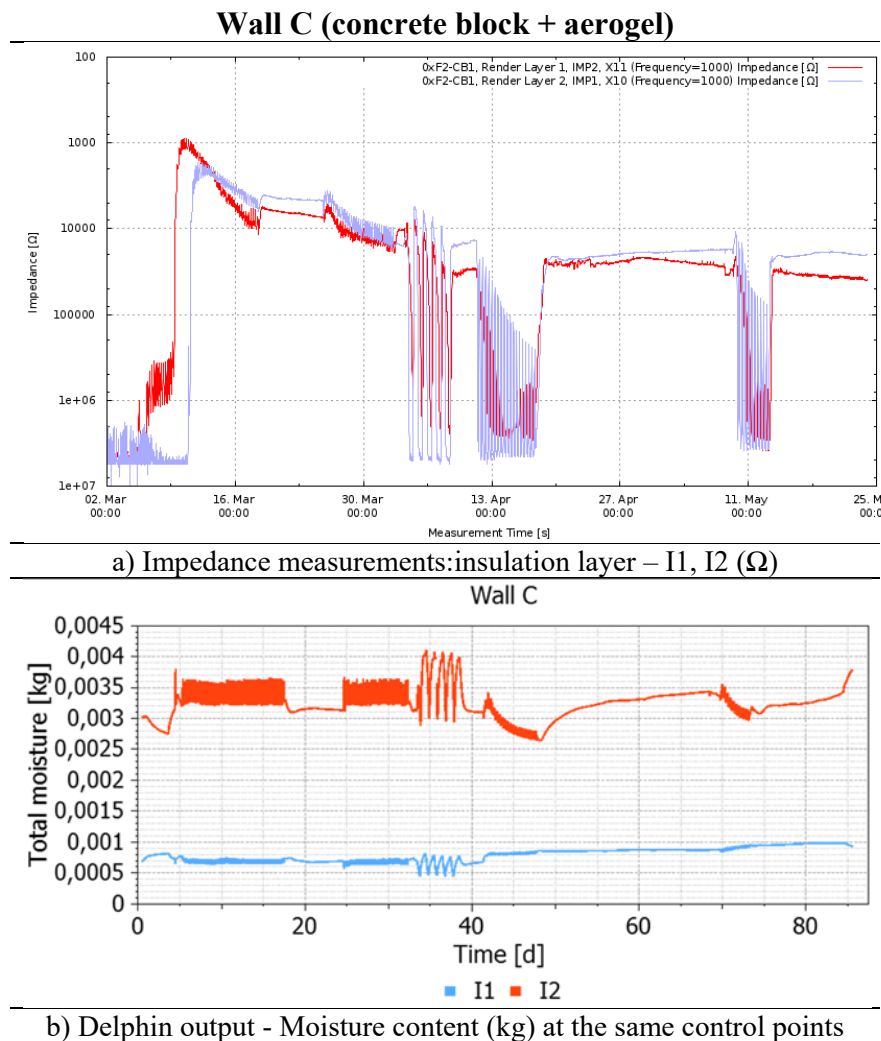*b) Simulated total moisture mass at the same control points*

Wall C (concrete block + aerogel)

a) Impedance measurements:insulation layer – I1, I2 (Ω)

b) Delphin output - Moisture content (kg) at the same control points
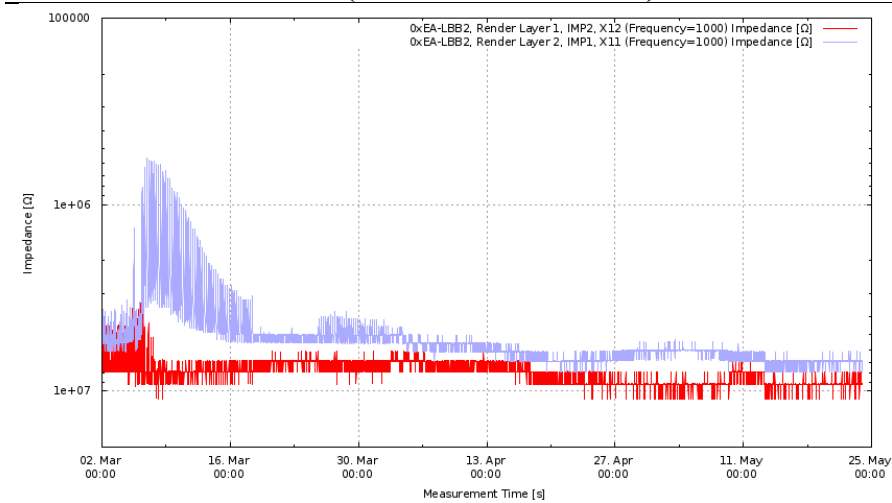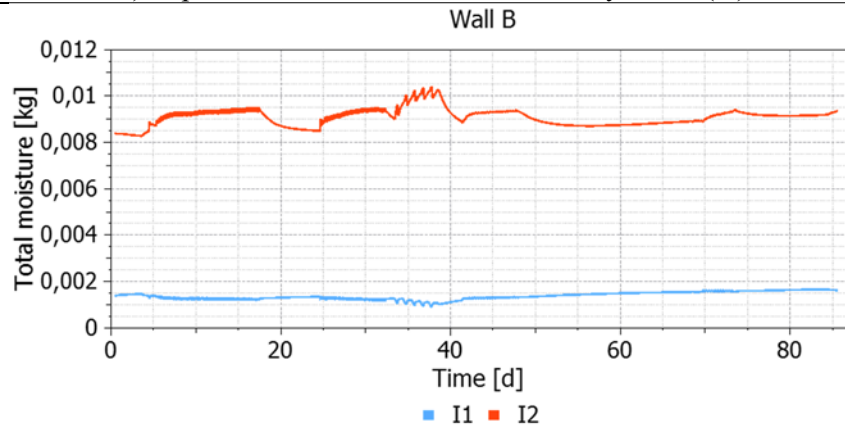
Fig. 6: Moisture content over time in Wall C. a) Impedance measurements I1, I2,
b) Simulated total moisture mass at the same control points

Both impedance and simulation results show higher moisture content close to the walls surfaces (I2 – dark line) as they hinder moisture and liquid transport, which end up accumulating in this interface. Only the impedance measurements of Wall B diverge from this pattern. The sensors installed on this wall, located on the right front of the test chamber, received less water during the wet cycles, remaining dry and therefore not "activated". The impedance at Wall B, especially for the sensor I2 is at the detection limit.

Wall B (brick + Tri-O-Therm)

a) Impedance measurements:insulation layer – I2 (Ω)

c) Delphin output - Moisture content (kg) at the same control point (I2)

Fig. 7: Moisture content over time in Wall B. a) Impedance measurements I1, I2, b) Simulated total moisture mass at the same control points
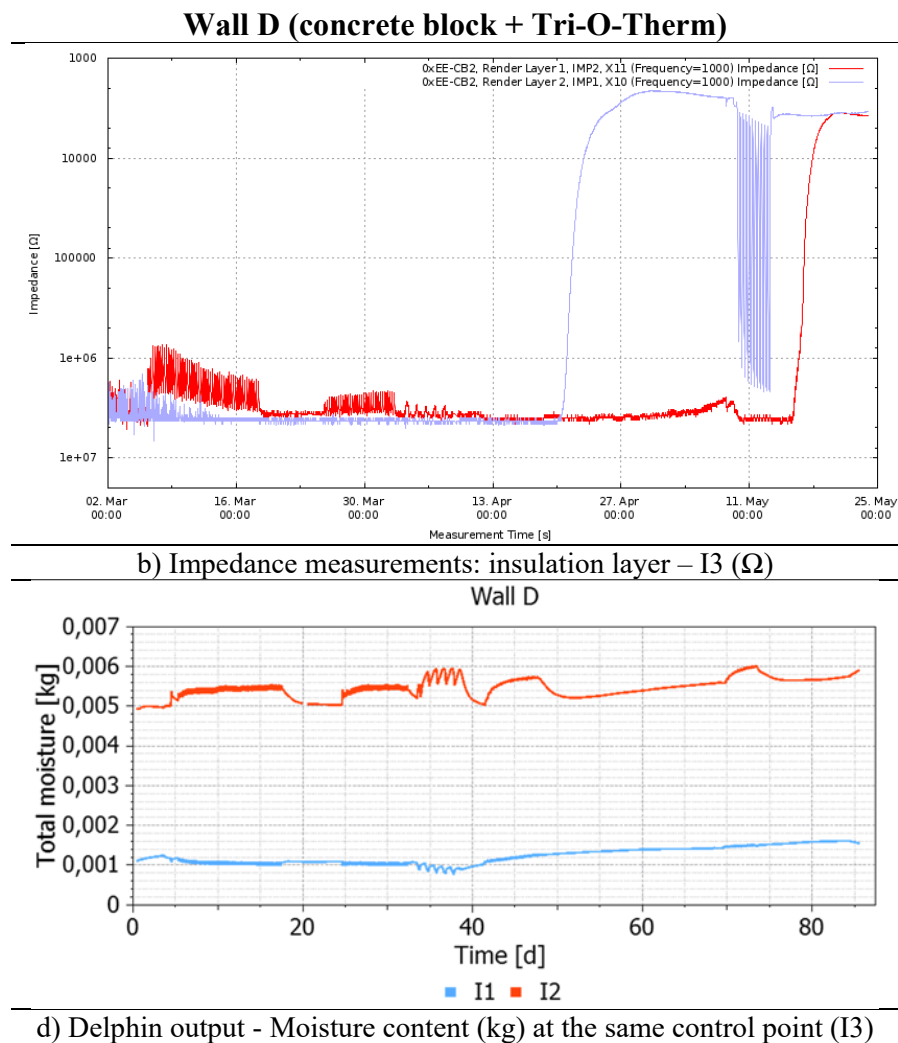
Wall D (concrete block + Tri-O-Therm)

b) Impedance measurements: insulation layer – I3 (Ω)

d) Delphin output - Moisture content (kg) at the same control point (I3)

*Fig. 8: Moisture content over time in Wall D. a) Impedance measurements I1, I2,
b) Simulated total moisture mass at the same control points*

Moreover, on all walls analyzed, the simulated values have more stable behaviour than the impedance measured. This difference is due to the intrusion of liquid water through small cracks and not optimal areas in the renders during the rain periods. Impedance in Walls A and C detected this humidity at the beginning of the test within the first rain period, while Wall D only by the end of the last rain period. Under ideal conditions, the finishing layer applied on the insulating plaster protects it from weathering, guaranteeing or prolonging its hygrothermal performance. However, temperature and humidity variation can generate cracks in this reinforcement, exposing the insulating layer to the external environment, which leaves it susceptible to water uptake. The variation in impedance at the observed depths portrays this scenario, showing changes in its measurements that correspond to an overhygroscopic state of the material. On the other hand, the simulation outputs did not reflect this particular situation.

Faced with such a scenario and despite the limitations highlighted, confronting the impedance measurements with the simulated total humidity of HMT models helped to understand the phenomena involving the hygrothermal performance of the components under ideal or extreme conditions. However, it should be noted that the relationships established here are strictly qualitative, and other investigations and tests are necessary to accomplish quantitative analyses.

Finally, the need for other control points besides those established in the test is emphasized. Installing sensors at different heights and positions on the evaluated walls and also monitoring the flow and water dispersion would allow a better characterization of the test, as well as better assistance when calibrating the numerical models.

ACKNOWLEDGEMENT

REFERENCES

[1]   EUROPEAN COMMISSION, *A policy framework for climate and energy in the period from 2020 to 2030*, 2014. https://eur-lex.europa.eu/legal-content/EN/TXT/PDF/?uri=CELEX:52014DC0015&from=EN (accessed 19 August 2020)

[2]   IBRAHIM, M., SAYEGH, H., BIANCO, L., WURTZ, E.: *Hygrothermal performance of novel internal and external super-insulating systems: In-situ experimental study and 1D/2D numerical modeling*, Applied Thermal Engineering 150 (2019) 1306–1327. https://doi.org/10.1016/j.applthermaleng.2019.01.054

[3]   LUCCHI, E., BECHERINI, F., DI TUCCIO, M.C., TROI, A., FRICK, J., ROBERTI, F., HERMANN, C., FAIRNINGTON, I., MEZZASALMA, G., POCKELÉ, L., BERNARDI, A.: *Thermal performance evaluation and comfort assessment of advanced aerogel as blown-in insulation for historic buildings*, Building and Environment 122 (2017) 258–268. https://doi.org/10.1016/j.buildenv.2017.06.019

[4]   Macher, J.M., Mendell, M.J., Chen, W., Kumagai, K.: *Development of a method to relate the moisture content of a building material to its water activity*, Indoor Air 27 (2017) 599–608. https://doi.org/10.1111/ina.12346

[5]   Ibrahim, M., Biwole, P.H., Wurtz, E., Achard, P.: *A study on the thermal performance of exterior walls covered with a recently patented silica-aerogel-based insulating coating*, Building and Environment 81 (2014) 112–122. https://doi.org/10.1016/j.buildenv.2014.06.017

[6]   Chang, S.J., Kim, S.: *Hygrothermal performance of exterior wall structures using a heat, air and moisture modeling*, Energy Procedia 78 (2015) 3434–3439. https://doi.org/10.1016/j.egypro.2015.12.328

[7]   Delgado, J.M.P.Q., de Freitas, V.P., Ramos, N.M.M., Barreira, E.: *Numerical simulation of exterior condensations on façades: The Undercooling Phenomenon*, ASHRAE (2010)

[8]   Ibrahim, M., Wurtz, E., Biwole, P.H., Achard, P., Sallee, H.: *Hygrothermal performance of exterior walls covered with aerogel-based insulating rendering*, Energy and Buildings 84 (2014) 241–251. https://doi.org/10.1016/j.enbuild.2014.07.039

[9]   Marincioni, V., Altamirano-Medina, H., Ridley, I.: *Performance of internal wall insulation systems - experimental test for the validation of a hygrothermal simulation tool*, in: NSB 2014: 10th Nordic Symposium on Building Physics: Full papers., Lund, Sweden, 2014, pp. 119–126

[10]   Busser, T., Piot, A., Pailha, M., Bejat, T., Woloszyn, M.: F*rom materials properties to modelling hygrothermal transfers of highly hygroscopic walls*, in: Proceedings of the CESBP Central European Symposium on Building Physics And BauSIM 2016, Dresden, Germany, 2016, pp. 767–774

[11]   Busser, T., Berger, J., Piot, A., Pailha, M., Woloszyn, M.: *Comparison of model numerical predictions of heat and moisture transfer in porous media with experimental observations at material and wall scales: An analysis of recent trends*, Drying Technology 37 (2019) 1363–1395. https://doi.org/10.1080/07373937.2018.1502195

[12]   Johansson, P., Geving, S., Hagentoft, C.-E., Jelle, B.P., Rognvik, E., Kalagasidis, A.S., Time, B.: I*nterior insulation retrofit of a historical brick wall using vacuum insulation panels: Hygrothermal numerical simulations*

and laboratory investigations, Building and Environment 79 (2014) 31–45. https://doi.org/10.1016/j.buildenv.2014.04.014

[13] FREUDENBERG, P., RUISINGER, U., STÖCKER, E.: *Calibration of hygrothermal simulations by the help of a generic optimisation tool*, Energy Procedia 132 (2017) 405–410. https://doi.org/10.1016/j.egypro.2017.09.645

[14] WALL-ACE PROJECT, 2017-2019. https://www.wall-ace.eu/ (accessed 21 August 2020)

[15] DIN EN 16383: *Thermal insulation products for building applications – Determination of the hygrothermal behaviour of external thermal insulation composite systems with renders*, 2017

[16] SAKIYAMA, N.R.M., FRICK, J., GARRECHT, H.: *Determination of U-values of render systems supposed to weathering*, Otto-Graf-Journal 18 (2019) 273–284

[17] B.C. BAUKLIMATIK DRESDEN, Delphin: Simulation program for the calculation of coupled

[18] DIN EN 15026 *Hygrothermal performance of building components and building elements – Assessment of moisture transfer by numerical simulation*, 2007

[19] FANTUCCI, S., FENOGOLIO, E., SERRA, V., PERINO, M.: *Coupled heat and moisture transfer simulations on building components retrofitted with a newly developed aeroge-based coating*, in: Proceedings of Building Simulation 2019: 16th Conference of IBPSA, Rome, Italy, 2019

[20] HARRESTRUP, M., SVENDSEN, S.: *Internal insulation applied in heritage multi-storey buildings with wooden beams embedded in solid masonry brick façades*, Building and Environment 99 (2016) 59–72. https://doi.org/10.1016/j.buildenv.2016.01.019

[21] DIN EN 12667 *Thermal performance of building materials and products – Determination of thermal resistance by means of guarded hot plate and heat flow meter methods – Products of high and medium thermal resistance*, 2001

[22] ASTM C1784-20, *Standard Test Method for Using a Heat Flow Meter Apparatus for Measuring Thermal Storage Properties of Phase Change Materials and Products*, West Conshohocken, PA, 2020

[23] DIN EN 1602 *Thermal insulating products for building applications – Determination of the apparent density*, 2013

[24] DIN EN 8130-2 *Coating powders - Part 2: Determination of density by gas comparison pyknometer (referee method)*, 2010

[25] DIN EN ISO 12572 *Hygrothermal performance of building materials and products – Determination of water vapour transmission properties – Cup method*, 2016

[26] DIN EN 1015-18 *Methods of test for mortar for masonry - Part 18: Determination of water absorption coefficient due to capillary action of hardened mortar*, Germany, 2002

[27] ASHRAE, Guideline 14-2002: *Measurement of energy and demand savings, society of Heating, refrigerating and air-conditioning engineers*